The climate impact of ship NO_x emissions: an improved estimate accounting for plume chemistry

C. D. Holmes[1], M. J. Prather[1], G. C. M. Vinken[2]

[1] Department of Earth System Science, University of California, Irvine, USA

[2] Department of Applied Physics, Eindhoven University of Technology, Eindhoven, The Netherlands

Correspondence to C.D. Holmes (cdholmes@uci.edu)

Abstract

Nitrogen oxide (NO_x) emissions from maritime shipping produce ozone (O_3) and hydroxyl radicals (OH), which in turn destroy methane (CH_4). The balance between this warming (due to O_3) and cooling (due to CH_4) determines the net effect of ship NO_x on climate. Previous estimates of the chemical impact and radiative forcing (RF) of ship NO_x have generally assumed that plumes of ship exhaust are instantly diluted into model grid cells spanning hundreds of kilometers, even though this is known to produce biased results. Here we improve the parametric representation of exhaust-gas chemistry developed in the GEOS-Chem chemical transport model (CTM) to provide the first estimate of RF from shipping that accounts for sub-grid-scale ship plume chemistry. The CTM now calculates O_3 production and CH_4 loss both within and outside the exhaust plumes and also accounts for the effect of wind speed. With the improved modeling of plumes, ship NO_x perturbations are smaller than suggested by the ensemble of past global modeling studies, but if we assume instant dilution of ship NO_x on the grid scale, the CTM reproduces previous model results. Our best estimates of the RF components from increasing ship NO_x emissions by 1 Tg(N) yr^{-1} are smaller than given in the past literature: $+3.4 \pm 0.85$ mW m^{-2} (1-σ confidence interval) from the short-lived ozone increase, -5.7 ± 1.3 mW m^{-2} from the CH_4 decrease, and -1.7 ± 0.7 mW m^{-2} from the long-lived O_3 decrease that accompanies the CH_4 change. The resulting net RF is -4.0 ± 2.0 mW m^{-2} for emissions of 1 Tg(N) yr^{-1}. Due to non-linearity in O_3 production as a function of background NO_x, RF from large changes in ship NO_x emissions, such as the increase since preindustrial times, is about 20% larger than this RF value for small marginal emission changes. Using sensitivity tests in one CTM, we quantify sources of uncertainty in the RF components and causes of the ±30% spread in past model results. The main source of uncertainty is the composition of the background atmosphere in the CTM, which is driven by model formulation (±10 to 20%) and the plausible range of anthropogenic emissions (±10%).

1. Introduction

Maritime shipping affects climate through emissions of CO_2, nitrogen oxides ($NO_x \equiv NO+NO_2$), and SO_2, the latter two of which indirectly influence methane, ozone, aerosols, and clouds. Other climate impacts due to ship emissions of CO, volatile organic compounds (VOCs), and primary aerosols have significant uncertainties, but are much smaller (Eyring et al., 2010). While ships produce only 3% of anthropogenic CO_2, they emit 17% of anthropogenic NO_x and 10% of anthropogenic SO_2 due to high engine temperatures and efficiencies, use of high-sulfur fuel, and general lack of emission controls (Lamarque et al., 2010). CO_2 unambiguously warms the climate and sulfate aerosol derived from SO_2 unambiguously cools it; the net forcing from NO_x, however, involves both warming and cooling components. NO_x emissions, whether from ships or other sources, favor ozone production (warming) as well as hydroxyl (OH) production that destroys methane (cooling). The net balance of these competing effects is cooling for most ground-based NO_x emission sources, including ships (e.g. Fiore et al., 2012), but can be warming for aviation NO_x (Holmes et al., 2011). Here, we summarize all previous reports of methane and ozone radiative forcing (RF) from ship NO_x and then calculate an improved RF that accounts for non-linear chemistry in the exhaust plumes.

Rapidly growing international trade has spurred rising ship traffic in recent decades, maintaining around 4% annual growth in the 2000s decade, with important impacts on air quality as well as climate (Dalsøren et al., 2010; Eyring et al., 2010). Ozone generated by increased shipping may explain much of the observed rise in background ozone concentrations reported at coastal sites (Chan, 2009; Dalsøren et al., 2010; Parrish et al., 2009). Holmes et al. (2013) found that rising ship NO_x emissions since 1980 have been one of the most important drivers of decreasing atmospheric methane lifetime and that the wide range of modeled sensitivities to ship emissions is one of the larger uncertainties in calculating trends in methane lifetime. These ship emissions and impacts on climate and air quality are projected to continue growing rapidly through the coming decades unless major changes in emission control technology are adopted (Corbett et al., 2010; Dalsøren et al., 2013; Eyring et al., 2005a; Hodnebrog et al., 2011; Koffi et al., 2010; Paxian et al., 2010).

Early efforts to include ship NO_x emissions in global 3-D chemical transport models (CTMs) found that NO_x concentrations were severely overestimated (Davis et al., 2001; Kasibhatla et al., 2000). Subsequent work indicated that the problem was not caused by emission inventory errors, but instead arose from the expedient but inaccurate modeling assumption that ship exhaust instantly mixes into a model grid cell, which is typically hundreds of kilometers across. Under

this instant dilution assumption coarse-resolution models bypass the early stages of plume dilution when high NO_x concentrations intensify NO_x chemical losses and suppress O_3 formation several fold (Chen et al., 2005; Kim et al., 2009; Song et al., 2003). While the non-linear nature of NO_x-HO_x-O_3 chemistry in plumes is well known (e.g. Lin et al., 1988) and numerical techniques have been developed for modeling sub-grid-scale plumes from other sources (e.g. Paoli et al., 2011; Sillman et al., 1990), many global CTMs have continued to use the instant dilution assumption for ship NO_x while acknowledging its deficiency. As a result, these models overestimate O_3 and OH production by ships and generate biased impacts on climate and air quality. To date, all estimates of RF due to ship NO_x come from models that assume instant dilution (Eyring et al., 2010).

Large-eddy simulations at various spatial resolutions suggest the errors in surface O_3 and OH enhancements caused by instant dilution of ship emissions in global CTMs are as large as 60% (Charlton-Perez et al., 2009), although some Gaussian plume models find larger errors in Northern Hemisphere shipping corridors (Franke et al., 2008; von Glasow et al., 2003). In a European regional CTM, parameterizing ship plume chemistry reduces ship-caused surface O_3 by 20% over the North Atlantic Ocean and more near coasts, as compared to instant dilution (Huszar et al., 2010). Vinken et al. (2011; 2013), using a different plume-in-grid approach in the GEOS-Chem global CTM, found similar magnitude reductions in O_3 and also showed that the parameterization improved the model's agreement with NO_x observations across several ocean basins.

In this paper we further develop the plume parameterization in GEOS-Chem to better represent CH_4 oxidation within ship exhaust plumes. We then calculate the global impact of ship NO_x on abundances of O_3 and CH_4 and on RF. These impact estimates change under different plume modeling assumptions and accounting for sub-grid-scale chemistry reduces the RF of ship NO_x compared to the ensemble of past studies. We also identify major sources of uncertainty in ship NO_x RF using similar methods to our earlier work on aviation NO_x (Holmes et al., 2011): by decomposing the RF into factors that can be assessed individually and by reproducing the spread of past results in a single model.

2. Model description

GEOS-Chem is a global tropospheric CTM driven by assimilated meteorological data from the NASA Goddard Earth Observing System (GEOS-5) (Rienecker et al., 2008). The version

used here (9-01-03, www.geos-chem.org) has 2° × 2.5° horizontal resolution and 47 layers. The tropospheric chemical mechanism simulates HO_x-NO_x-VOC-O_3 reactions, including bromine (Parrella et al., 2012). Anthropogenic emissions are based on the EDGAR and RETRO global inventories (Olivier and Berdowski, 2001; van Aardenne et al., 2005; van Donkelaar et al., 2008; van het Bolscher, 2008), which are replaced with regional inventories over the United States (NEI2005), Canada (CAC), Mexico (BRAVO), Europe (EMEP) and East Asia (Streets). Ship emissions are described further below.

Figure 1 shows ship NO_x emissions in GEOS-Chem which are 5.0 Tg(N) yr^{-1} and distributed according to ship locations in the AMVER-ICOADS database for each month (Lee et al., 2011; Wang et al., 2008). This is close to the best estimate of 5.4 Tg(N) yr^{-1} for year 2000 (Eyring et al., 2010), and well within the plausible range of 3.0-10.4 Tg(N) yr^{-1} (Corbett and Koehler, 2003; Endresen et al., 2007; 2003; Eyring et al., 2005b). GEOS-Chem also includes ship emissions of SO_2 (8.5 Tg(S) yr^{-1}; Eyring et al., 2005b), CO (1.1 Tg yr^{-1}; Wang et al., 2008), and VOCs, although ship CO and VOCs are small compared to other sources of those gases. We quantify the effects of ship emissions by comparing a simulation with the base inventory to one with a uniform 5% increase in ship NO_x emissions and another with zero ship NO_x emissions. Results are derived from a simulation of year 2006 after spin up from July 2005.

2.1 Plume chemistry and dispersion

Previous versions of GEOS-Chem assumed that sub-grid chemistry in ship plumes convert each mole of NO_x emissions into 10 mole of O_3 and 1 mole of HNO_3—an ozone production efficiency (OPE) of 10—based on observations of aged ship plumes (Chen et al., 2005). Imposing a globally constant effective emission factor obviously neglects diurnal, seasonal, and regional influences on plume chemistry. In addition, using this method underestimates NO_x concentrations in ship tracks, since some NO_x survives oxidation until the plume has expanded to the global grid resolution. To redress these shortcomings, Vinken et al. (2011) used a Gaussian plume chemistry model to calculate the dilution and chemical evolution of the exhaust over 5 hours, at which point the plume approximately fills a grid cell in the global CTM. The final OPE and fraction of NO_x oxidized to HNO_3 are tabulated for various environmental conditions in a look-up table that GEOS-Chem uses to determine locally appropriate emission factors for ship NO_x, O_3, and HNO_3. These aged plume emissions are then injected into the global CTM, which then accounts for the subsequent grid-scale photochemistry and large-scale advection. Although Gaussian plume models poorly simulate the first several minutes of plume aging, when turbulent transport limits

the rates of fast NO_x-O_3 chemical reactions (Galmarini et al., 1995; Sykes et al., 1992), they can provide a good representation of plume composition after about ten minutes (several kilometers) of aging, once turbulent dispersion homogenizes the plume (Galmarini et al., 1995). Indeed Vinken et al. (2011) demonstrated that their Gaussian plume model predicts NO_x, O_3, and OH concentrations consistent with field observations over several hours of ship plume aging (Chen et al., 2005).

In this work, we update the Gaussian plume model to calculate CH_4 oxidation within the ship plume and verify that the updated model still reproduces field observations of NO_x, O_3, and OH concentrations (Fig. S1). We also add wind speed as a factor in the look-up table, since CH_4 oxidation and O_3 production can vary by a factor of 2 between wind speeds of 2 and 18 m s^{-1}. Our updated plume-in-grid parameterization depends on 8 meteorological and chemical factors: ambient concentrations of NO_x and O_3, solar zenith angle at emission time and 5 hours later, photolysis rates of NO_2 and O_3, temperature, and wind speed. Figure S2 shows how the parameterization responds to each of these factors. Clouds affect the parameterized plume chemistry through photolysis rates, but not through dispersion rates (Verzijlbergh et al., 2009). The global CTM with updated plume chemistry has up to 3% less NO_x and 1% less O_3 in the marine boundary layer compared to the earlier parameterization. Therefore, comparisons of the CTM to observations over the North Atlantic and North Pacific Oceans shown by Vinken et al. (2011; their Figs. 4,5) are unchanged. Specifically, in regions that are impacted by ship emissions but outside distinct plumes, the parametric plume chemistry predicts median NO_x abundances within 30% of observed values while instant dilution over predicts NO_x by a factor of 2. Ozone observations in the same regions are consistent with the plume parameterization but unable to falsify other model variants.

We compare the chemical and climate impact of shipping under three different modeling assumptions about plume dilution and chemistry:

1. Instant dilution. We neglect sub-grid chemistry and emit NO_x into the CTM grid, at the rate specified by the emission inventory, as done in previous studies with other models.

2. Fixed OPE. We assume that sub-grid chemistry converts each mole of ship NO_x to 10 moles of O_3 and 1 mole of HNO_3.

3. Parametric plume chemistry. This is our best representation of sub-grid plume chemistry using the lookup tables described above.

2.2 Radiative forcing calculations

The global mean RF (F) from ship NO_x emissions consists of a short-lived O_3 component (F_{O3}) that decays within months after emissions and long-lived CH_4 and O_3 components that persist for over a decade (F_{CH4} and $F_{long\text{-}O3}$, respectively):

$$F = F_{O3} + F_{CH4} + F_{long\text{-}O3}. \quad (1)$$

We calculate these components in steady state from the CTM output using a similar decomposition as Holmes et al. (2011):

$$F_{O3} = (d[O_3]/dE)\,(dF/d[O_3])\,\Delta E, \quad (2)$$

$$F_{CH4} = (d \ln \tau_{total}/dE)\, f\, [CH_4]\, (dF/d[CH_4])\, S\, \Delta E, \text{ and} \quad (3)$$

$$F_{long\text{-}O3} = a\, F_{CH4} / S, \quad (4)$$

where $d[O_3]/dE$ is the steady-state response to ship NO_x emissions (E) while holding $[CH_4]$ constant and $d \ln \tau_{total}/dE$ is the accompanying change in total atmospheric CH_4 lifetime, $dF/d[O_3]$ and $dF/d[CH_4]$ are the radiative efficiencies of tropospheric O_3 and CH_4, $[CH_4] = 1.76$ ppm is the global-mean CH_4 mole fraction in 2000, f is the CH_4 feedback factor that prolongs the lifetime of CH_4 perturbations, $S = 1.15$ is the enhancement of F_{CH4} due to CH_4-derived stratospheric water vapor (Myhre et al., 2007), and $a = 0.34 \pm 0.13$ describes the perturbations to O_3 abundance and RF that accompany global CH_4 changes. The a term derives from a literature survey of multiple CTMs and radiative transfer models (see SI and Holmes et al. 2011). This CTM and most prior publications report changes in the CH_4 lifetime due to tropospheric OH (τ) rather than the total atmospheric lifetime; these are related via $(d \ln \tau_{total}) = b\, (d \ln \tau)$, where the best estimates of all atmospheric methane losses imply $b = 0.82 \pm 0.03$ (Prather et al., 2012).

CTM diagnostics provide $d[O_3]/dE$ and $d \ln \tau/dE$ for each plume chemistry treatment based on 5% perturbations to global ship NO_x emissions. Values and one-sigma (68%) confidence intervals for other factors in equations 2-4 are given in Holmes et al. (2011), with the following updates. Recent data suggest a smaller feedback factor, $f = 1.34 \pm 0.06$ (Holmes et al., 2013). We use a ship-specific radiative efficiency for O_3, which is smaller than that of aviation O_3 and that of long-lived O_3 changes (cf. Fuglestvedt et al., 2008; Holmes et al., 2011) because ship O_3 is mostly confined to low altitudes and high latitudes (e.g. Hoor et al., 2009). We adopt a value of 33 ± 4 mW m^{-2} DU^{-1}, based on the mean of recent studies (Table 1; Hoor et al., 2009; Myhre et al., 2011), recognizing that radiative efficiency depends on the distribution of the O_3 burden and that radiative transfer models differ by about 10% (Myhre et al., 2011). While models assuming

instant dilution of ship NO_x were used to calculate the ozone radiative efficiency, we show below that the pattern of ship ozone perturbations is similar with the parametric plume assumption.

3. Chemical response to ship NO_x emissions

3.1 Ozone production

Figure 2 shows simulated, time-averaged OPE of ship NO_x with parametric plume chemistry. OPE is defined here as $\Delta P(O_x) / \Delta L(NO_x)$, where P(X) and L(X) are the time-integrated production and loss of species X, O_x is the odd oxygen family ($O + O_3 + NO_2 + 2NO_3$ + many reservoirs of NO_2 and NO_3, see e.g. Parrella et al., 2012), and Δ refers to a steady-state change caused by a 5% increase in ship NO_x emission. Chemical oxidation to HNO_3 and nitrate is the main NO_x loss process, but surface deposition of NO_2, N_2O_5 and organic nitrates are about 6% of global $L(NO_x)$ and 2% of $\Delta L(NO_x)$. The parametric plume chemistry calculates a global-mean OPE of 1.7 during young plumes. Some ship NO_x survives beyond the 5-hour scope of the plume parameterization and its subsequent chemical effects are calculated with the grid-resolved chemistry. The global-mean total OPE (plume plus grid chemistry) is 8.5. Although OPE is negative at night and episodically in polluted continental outflow, the annual-mean OPE is positive everywhere, both in the first 5 hours and total. The busiest shipping corridors in the North Atlantic and North Pacific Oceans have an OPE of 4-8 while values around 40 are found in the least-trafficked areas of the Equatorial Pacific Ocean. Figure 3 shows zonal-mean OPE for the other plume assumptions. With the instant dilution assumption OPE is 12.5. Thus, the parametric plume chemistry has the intended effect of suppressing O_3 production by 30%, relative to instant dilution. The fixed OPE scenario assumes OPE to be 10 in the plume, but subsequently global O_3 production is suppressed in grid-resolved chemistry since no NO_x is released so the total OPE is 8.0.

O_3 enhancements generated by ship NO_x concentrate over the major emission regions in the Atlantic and Pacific Oceans and a narrow strip in the Indian Ocean, as seen in Figure 4. The largest O_3 enhancements are displaced eastward relative to the emissions in each ocean basin, as found in previous studies, reflecting cumulative downwind production (Endresen et al., 2003; Eyring et al., 2007). Figure 3 compares the zonal-mean O_3 column enhancements across the three plume chemistry simulations. The pattern is similar in the instant dilution and parametric plume simulations and this justifies our use of O_3 radiative efficiencies that were derived in models with instant dilution. O_3 column enhancements in the fixed OPE simulation are qualitatively different

and concentrated mainly in the high northern latitudes, because OPE is not suppressed in winter or by high NO_x emissions in this scenario. As Table 2 reports, the global-mean O_3 column change for a 1 Tg(N) yr^{-1} increase in ship NO_x is 0.10 DU in the parametric plume model, compared to 0.16 DU under the instant dilution assumption and 0.12 DU under fixed OPE assumption. These column perturbations are not strictly proportional to the OPE across scenarios because the lifetime of O_3 increases towards the poles. Previous CTM studies using instant dilution found 0.14-0.2 DU enhancements for emissions of 1 Tg(N) yr^{-1} (Hodnebrog et al., 2011; Hoor et al., 2009), which encompasses our estimate under instant dilution.

3.2 Methane oxidation

NO_x emissions affect OH concentrations and CH_4 oxidation in two general ways: directly by recycling HO_2 and RO_2 back to OH, which increases the OH/HO_2 ratio and reduces the HO_x sink via HO_2 self reaction; and indirectly by increasing O_3, which is a primary source of OH through photolysis in the presence of water vapor. We define a time-averaged CH_4 oxidation efficiency (MOE) similar to OPE above, as $\Delta L(CH_4) / \Delta L(NO_x)$. The MOE is 0.42 in the first 5 hours of plume aging, as calculated by the parametric plume chemistry (Figure 2). MOE is low in the young plume because of rapid NO_x loss, despite high OH concentrations in the plume that can be double the ambient values (Chen et al., 2005; Song et al., 2003). The NO_x lifetime and MOE increase in the grid-scale chemistry, so that the total MOE is 3.1 with parametric plume chemistry. The instant dilution assumption raises the overall MOE to 4.4, while in the fixed OPE simulation the MOE is only 1.2 because the direct chemical effects of ship NO_x on OH are neglected.

Table 3 reports the sensitivity of CH_4 lifetime to increasing ship NO_x emissions by 1 Tg(N) yr^{-1}. The largest response occurs under instant dilution (-1.0%) and the smallest under fixed OPE (-0.26%), with the parametric plume falling in the middle (-0.7%). The instant dilution value is similar to those that we previously found in the University of California, Irvine (UCI) CTM and Oslo CTM3, -0.8% and -0.9%, respectively (Holmes et al., 2013) and within the range of values in literature (-0.9 ± 0.3%, Table 3). In past studies, the largest CH_4 lifetime changes per Tg(N) yr^{-1} (-1.3 to -1.4%) derived from models that used small inventories of ship emissions and calculated sensitivities by removing all ship NO_x emissions (Endresen et al., 2003; Lawrence and Crutzen, 1999). This suggests that the non-linear aspects of NO_x-ozone chemistry influence the spread of model results and we investigate this further in Section 4.

Treatment of ship plume chemistry has an important effect on the current CH_4 lifetime, as well as its perturbations (Table 3). In many CTMs, the CH_4 lifetime due to tropospheric OH is shorter than observed and the cause of this discrepancy remains unknown (e.g. Holmes et al., 2013; Naik et al., 2013). We find that instant dilution produces the shortest CH_4 lifetime of the three plume chemistry scenarios (9.2 yr). The more realistic treatment of ship plume chemistry afforded by the parametric plume model raises the lifetime to 9.4 yr, but the discrepancy with observations remains (Prather et al., 2012). While the fixed OPE model is longer (9.7 yr), it cannot be considered more realistic. Neglecting all ship NO_x emissions, the CH_4 lifetime is 9.8 yr. Thus, with parametric plume chemistry, ship NO_x drives about 4% of all CH_4 oxidation by tropospheric OH and 13% of that occurs in the first 5 hours of plume aging. Our results here include bromine chemistry, which acts as an O_3 and HO_x sink. Removing bromine chemistry from a simulation with fixed OPE shortens the CH_4 lifetime by about 0.5 yr, but the chemical impact of ship emissions is nearly unchanged from the values in Tables 2 and 3.

4. Radiative forcing from ship NO_x emissions

Figure 5 shows all past reports of the CH_4 and short-lived O_3 RF components from ship NO_x emissions. These include CTMs (Dalsøren et al., 2010; 2013; 2009; 2007; Eide et al., 2013; Endresen et al., 2003; Eyring et al., 2007; Fuglestvedt et al., 2008; Hodnebrog et al., 2011; Hoor et al., 2009; Lawrence and Crutzen, 1999; Myhre et al., 2011) and global climate models with chemistry (Eyring et al., 2007; Hoor et al., 2009; Myhre et al., 2011; Olivie et al., 2012; Unger et al., 2010), as well as some derived from literature synthesis (Borken-Kleefeld et al., 2010; Lee et al., 2007). Where possible, we calculate F_{CH4} from the reported changes in CH_4 lifetime using Eq. (3), in order to use consistent assumptions about CH_4 lifetime, feedback and radiative efficiency. RF values are scaled to emissions of 1 Tg(N) yr^{-1} and are for steady-state conditions. We report results from individual models in multi-model studies where possible. All of these RF estimates have assumed instant dilution of ship emissions, which biases the RF values as we show below.

From the literature ensemble, we estimate the O_3 RF to be +6.0 ± 1.9 mW m^{-2} and the CH_4 RF to be -8.0 ± 2.4 mW m^{-2} for 1 Tg(N) yr^{-1}. This average neglects two studies with small absolute magnitudes that were clearly related to unjustified modeling assumptions. Early work by Lee et al. (2007) used CH_4 and O_3 sensitivities to land NO_x emissions, rather than ship-specific sensitivities that tend to be higher. The ship emission inventory used by one multi-model study (Eyring et al., 2007) was subsequently found to unrealistically concentrate ship emissions along narrow corridors and underestimate emissions in the tropics, as acknowledged in their work, both

of which tend to underestimate O_3 production. Figure 5 also shows three RFs estimates derived from our previous analysis of CH_4 lifetime (Holmes et al., 2013). Two of these estimates lie within the cluster of literature values and are based on CTMs that assume instant dilution, while the outlying third estimate based on an earlier version of GEOS-Chem with fixed OPE demonstrates that plume chemistry significantly influences the climate impact of ships.

In this work, the short-lived O_3 and CH_4 RFs with parametric plume chemistry are +3.4 and -5.7 mW m^{-2}, respectively, for emissions of 1 Tg(N) yr^{-1}. With instant dilution, the RF components are close to the central estimate from past literature and about 40% larger than our best estimate: +5.3 and -8.5 mW m^{-2}. The fixed OPE model, unlike the others, predicts that warming from short-lived O_3 (+3.8 mW m^{-2}) exceeds the CH_4 cooling (-2.2 mW m^{-2}) because instantly converting NO_x emissions to HNO_3 neglects its direct effect on OH. The radiative efficiency in the fixed OPE model is likely smaller than assumed here (see Sect. 2.3 and 3.1), but we have not recalculated it because the fixed OPE model is not used to derive our best estimate.

Global aerosol impacts of ship NO_x have been identified as a knowledge gap that we briefly estimate (Eyring et al., 2010). Ship NO_x increases oxidative production of nitrate and sulfate in our simulations by 9% and 0.4%, respectively, compared to a simulation with no ship NO_x. Some of these products absorb onto sea-salt aerosols, but this makes a negligible contribution to sea-salt aerosol mass, so no RF is expected. The largest changes in aerosol column concentration occur over land, however, due to long-range transport of O_3 and H_2O_2 perturbations from ship NO_x. These oxidants mainly convert SO_2 to sulfate in cloud water, which is quickly followed by wet deposition, so that ship NO_x drives sulfate aerosol burdens down over anthropogenic SO_2 source regions, despite the increased oxidation. Chemical teleconnections initiated by land-based NO_x emissions have been reported previously in which NO_x emissions increase sulfate burdens over distant continents (Leibensperger et al., 2011). Land-based and ship NO_x emissions may have opposite sign teleconnections with sulfate due to larger H_2O_2 perturbations produced in moist marine air, but these effects should be evaluated in other CTMs. Averaged globally, the sulfate burden falls by -6.3 μg m^{-2} for ship emissions of 1 Tg(N) yr^{-1}, and the nitrate burden increases by +7.9 μg m^{-2} to consume available ammonium. Applying radiative efficiencies (direct effect only) of these species (Myhre et al., 2013), the direct RF from these individual changes is +/- 1.2 mW m^{-2}, with nearly perfect cancellation between sulfate and nitrate components. The aerosol direct RF from ship NO_x is therefore only 2% of the O_3 and CH_4 RF. Aerosol indirect effects, black carbon, and organic carbon also contribute to radiative forcing from ships (Eyring et al., 2010) but are beyond the scope of this study of ship NO_x.

Our global RF calculation using parametric plume chemistry is the first to account for sub-grid-scale ship NO_x chemistry. Being based on a single model, we are unable to estimate uncertainties using the common approach of model ensembles. Instead we develop confidence intervals by propagating uncertainties through Eqs. (2)-(3). Among the ensemble of models with instant dilution, the one-sigma ranges of $(d[O_3]/dE)$ and $(d \ln \tau_{total}/dE)$ are 20% of their respective means. Assuming the same proportional uncertainty for these factors with parametric plume chemistry, and the one-sigma ranges for other factors given in Section 2.2, the one-sigma confidence intervals for CH_4 and short-lived O_3 RFs are 22% and 25%, respectively.

An alternative approach to uncertainty analysis is to probe the causes for spread among the past model studies. Much of this spread can be reproduced through several variants of the GEOS-Chem model, which are shown in Figure 5. Given the non-linear nature of NO_x-O_3 chemistry, we recalculate the ship NO_x RF against a reference simulation without any ship NO_x. To this point, all results derived from 5% emission perturbations, which describes the climate response to small marginal increases or decreases in emissions. Removing all ship NO_x from the simulation reveals the average RF of all ship NO_x and is a common way to calculate the ship NO_x RF since preindustrial times. With complete removal of ship NO_x, we find O_3 and CH_4 RF components per Tg(N) yr^{-1} are about 20% larger than with the 5% perturbations for both parametric plume chemistry and instant dilution. The RF components shift along the model ensemble's major axis of variability. Indeed past studies using complete removal have on average predicted 10% larger ship RF than studies with 5-30% emission perturbations, so combined effects of non-linearities and different perturbations might explain up to half of the model ensemble spread. We note that the RF components are insensitive to size of the ship NO_x perturbation when assuming fixed OPE. This demonstrates that the non-linear aspects of O_3 chemistry are generated almost entirely during NO_x loss and O_3 production, and that adding O_3 alone does not significantly change the O_3 lifetime.

Model grid resolution is known to influence climatically important chemical fluxes, such as O_3 production (Wild and Prather, 2006), so we test whether resolution affects RF from ship NO_x. Doubling the GEOS-Chem grid size to 4° × 5° reduces the CH_4 lifetime and O_3 burden compared to 2° × 2.5° resolution. Nevertheless, the O_3 and CH_4 responses to 5% increases in ship NO_x emissions are unchanged from the finer resolution. Given this resolution-independence, we conduct additional sensitivity tests at coarse resolution for computational expediency. A previous version of the model (9-01-02) differs by less than 10% in terms of ship-NO_x perturbations from the current version, despite improvements to wet scavenging, sea-salt aerosol, and stratospheric

chemistry (Jaeglé et al., 2011; Murray et al., 2012; Wang et al., 2011), indicating minimal sensitivity of ship NO_x impacts to these processes. The ship RF is quite sensitive to anthropogenic emissions, however. Using the Climate Model Intercomparison Project (CMIP5) inventory for year 2000 (Lamarque et al., 2010) rather than the standard inventory described in Section 2, the ship NO_x RF components are about 15% larger. The shift in RF components lies along the major axis of variability in the model ensemble, indicating global (not ship) inventory differences could contribute substantially to the ensemble spread presumably by generating background atmospheres with different levels of NO_x and HO_x precursors. The CMIP5 inventory prescribes more CO emissions (610 vs. 580 Tg(CO) yr^{-1}) and slightly less NO_x emissions (27.2 vs. 27.6 Tg(N) yr^{-1}) with large changes in their spatial distributions. These emission differences tend to reduce background OH and NO_x and make ozone production more NO_x sensitive, which is consistent with the direction of RF changes in the simulations. Our earlier work on climate forcing from aviation NO_x similarly identified background NO_x levels as a driver of model uncertainty. Although emission inventories are routinely updated and improved, reasonable inventories continue to differ by 10% for NO_x and 20% for CO at the global level; differences are often larger for biomass burning and natural emissions (Granier et al., 2011). If the two inventories in GEOS-Chem exhibit typical differences, then inventory uncertainty may account for ±10 % range in ship NO_x RF. Uncertainties in chemistry, transport and other processes that control background atmospheric composition contribute as much or more than emissions to the range in RF responses across models, since multi-model studies using common emissions still exhibit ±20 % ranges in RF components (e.g. Eyring et al., 2007; Hoor et al., 2009; Myhre et al., 2011). Three sources of uncertainty, when combined in quadrature, are therefore sufficient to explain the ±30 % range of ship RF components in the literature ensemble: non-linearity from the ship emission perturbation magnitude (±10 to 20%), emissions from other sources (±10%), and other processes that control background atmospheric composition (±10 to 20%).

5. Conclusions

The non-linear chemistry governing O_3 and OH production in emission plumes has been recognized for decades. In spite of this knowledge, global modeling studies of ship NO_x emissions and their impacts on climate and air quality are usually made under the assumption that emissions are instantly diluted into large grid volumes, which overestimates production of tropospheric O_3 and OH. We present a suite of model simulations that quantify this error, one of which uses an improved, more physically realistic treatment of plume chemistry on time and

spatial scales smaller than the global model grid. The limited observations of ship plume composition during aging hamper efforts to widely evaluate the parameterization, but we have shown that it is consistent with available data. With parametric plume chemistry, OPE from ship NO_x is 30% smaller than under instant dilution. Methane perturbations from ship NO_x are likewise reduced 30%. Parametric plume chemistry also increases the global atmospheric CH_4 lifetime compared to instant dilution, which brings the model closer to observations, bit it is still too short.

Our best estimate of the ship NO_x RF from the short-lived O_3 increase is +3.4 ± 0.85 mW m^{-2} for steady-state emissions of 1 Tg(N) yr^{-1}. The RF from the CH_4 decrease is -5.7 ± 1.3 mW m^{-2}, and RF from the long-lived O_3 reduction accompanying the CH_4 decrease is -1.7 ± 0.7 mW m^{-2}. For each component the central estimate is similar to the smallest magnitude of previously published RF estimates, due to our treatment of sub-grid-scale chemistry in ship emission plumes. Combining all these components and accounting for correlations caused by common factors, our best estimate of the total RF from ship NO_x is -4.0 ± 2.0 mW m^{-2}. Our RF estimate derives from marginal (5%) changes in ship NO_x emissions. Scaling the marginal RF up to year 2010 total emissions of 6.8 Tg(N) yr^{-1} (Eide et al., 2013) suggests an RF of -27.2 ± 13.6 mW m^{-2}, but the average RF of all ship NO_x emissions is likely about 20% larger (-33 mW m^{-2}) because of non-linearity in O_3 production. Our best estimates of individual RF components have one-sigma (68%) confidence intervals of ±20% to ±30%. The largest contribution to this uncertainty arises from differing abundances of photochemical oxidants in the background atmosphere, which when entrained into ship plumes can alter their chemistry. Global emissions and model formulation both contribute to these differences in the background atmosphere. Further reductions in RF uncertainty are therefore unlikely without stronger observational constraints on radical sources and sinks in the remote marine atmosphere and additional observational case studies of ship plume aging.

Acknowledgments

This research was supported by the NASA Modeling, Analysis, and Prediction Program (NNX13AL12G) and the Office of Science (BER) of the US Department of Energy (DE-SC0007021). Research at Eindhoven University of Technology was funded by the Netherlands Organization for Scientific Research, NWO Vidi grant 864.09.001. We also acknowledge helpful discussions with K.F. Boersma.

References

Borken-Kleefeld, J., Berntsen, T. and Fuglestvedt, J.: Specific climate impact of passenger and freight transport, Environ. Sci. Technol., 44(15), 5700–5706, doi:10.1021/es9039693, 2010.

Chan, E.: Regional ground-level ozone trends in the context of meteorological influences across Canada and the eastern United States from 1997 to 2006, J. Geophys. Res.-Atmos., 114, D05301, doi:10.1029/2008JD010090, 2009.

Charlton-Perez, C. L., Evans, M. J. and Marsham, J. H.: The impact of resolution on ship plume simulations with NOx chemistry, Atmos. Chem. Phys., 9, 7505–7518, 2009.

Chen, G., Huey, L., Trainer, M., Nicks, D., Corbett, J., Ryerson, T., Parrish, D., Neuman, J., Nowak, J., Tanner, D., Holloway, J., Brock, C., Crawford, J., Olson, J., Sullivan, A., Weber, R., Schauffler, S., Donnelly, S., Atlas, E., Roberts, J., Flocke, F., Hübler, G. and Fehsenfeld, F.: An investigation of the chemistry of ship emission plumes during ITCT 2002, J. Geophys. Res.-Atmos., 110, D10S90, doi:10.1029/2004JD005236, 2005.

Corbett, J. J. and Koehler, H. W.: Updated emissions from ocean shipping, J. Geophys. Res.-Atmos., 108(D20), 4650, doi:10.1029/2003JD003751, 2003.

Corbett, J. J., Lack, D. A., Winebrake, J. J., Harder, S., Silberman, J. A. and Gold, M.: Arctic shipping emissions inventories and future scenarios, Atmos. Chem. Phys., 10, 9689–9704, doi:10.5194/acp-10-9689-2010, 2010.

Dalsøren, S. B., Eide, M. S., Endresen, O., Mjelde, A., Gravir, G. and Isaksen, I. S. A.: Update on emissions and environmental impacts from the international fleet of ships: the contribution from major ship types and ports, Atmos. Chem. Phys., 9(6), 2171–2194, 2009.

Dalsøren, S. B., Eide, M. S., Myhre, G., Endresen, O., Isaksen, I. S. A. and Fuglestvedt, J. S.: Impacts of the large increase in international ship traffic 2000-2007 on tropospheric ozone and methane, Environ. Sci. Technol., 44(7), 2482–2489, doi:10.1021/es902628e, 2010.

Dalsøren, S. B., Endresen, O., Isaksen, I. S. A., Gravir, G. and Sorgard, E.: Environmental impacts of the expected increase in sea transportation, with a particular focus on oil and gas scenarios for Norway and northwest Russia, J. Geophys. Res.-Atmos., 112, D02310, doi:10.1029/2005JD006927, 2007.

Dalsøren, S. B., Samset, B. H., Myhre, G., Corbett, J. J., Minjares, R., Lack, D. and Fuglestvedt, J. S.: Environmental impacts of shipping in 2030 with a particular focus on the Arctic region, Atmos. Chem. Phys., 13(4), 1941–1955, doi:10.5194/acp-13-1941-2013, 2013.

Davis, D. D., Grodzinsky, G., Kasibhatla, P., Crawford, J., Chen, G., Liu, S., Bandy, A., Thornton, D., Guan, H. and Sandholm, S.: Impact of ship emissions on marine boundary layer NO_x and SO_2 distributions over the Pacific basin, Geophys. Res. Lett., 28(2), 235–238, 2001.

Eide, M. S., Dalsøren, S. B., Endresen, O., Samset, B., Myhre, G., Fuglestvedt, J. and Berntsen, T.: Reducing CO_2 from shipping – do non-CO_2 effects matter? Atmos. Chem. Phys., 13(8), 4183–4201, doi:10.5194/acp-13-4183-2013, 2013.

Endresen, O., Sorgard, E., Behrens, H. L., Brett, P. O. and Isaksen, I. S. A.: A historical

461 reconstruction of ships' fuel consumption and emissions, J. Geophys. Res.-Atmos., 112, D12301,
462 doi:10.1029/2006JD007630, 2007.

463 Endresen, O., Sorgard, E., Sundet, J. K., Dalsøren, S. B., Isaksen, I., Berglen, T. F. and Gravir,
464 G.: Emission from international sea transportation and environmental impact, J. Geophys. Res.-
465 Atmos., 108, 4560, doi:10.1029/2002JD002898, 2003.

466 Eyring, V., Isaksen, I. S. A., Berntsen, T., Collins, W. J., Corbett, J. J., Endresen, O., Grainger, R.
467 G., Moldanova, J., Schlager, H. and Stevenson, D. S.: Transport impacts on atmosphere and
468 climate: Shipping, Atmos. Environ., 44(37), 4735–4771, doi:10.1016/j.atmosenv.2009.04.059,
469 2010.

470 Eyring, V., Kohler, H. W., Lauer, A. and Lemper, B.: Emissions from international shipping: 2.
471 Impact of future technologies on scenarios until 2050, J. Geophys. Res.-Atmos., 110, D17306,
472 doi:10.1029/2004JD005620, 2005a.

473 Eyring, V., Kohler, H. W., van Aardenne, J. and Lauer, A.: Emissions from international
474 shipping: 1. The last 50 years, J. Geophys. Res.-Atmos., 110(D17), D17305,
475 doi:10.1029/2004JD005619, 2005b.

476 Eyring, V., Stevenson, D. S., Lauer, A., Dentener, F. J., Butler, T., Collins, W. J., Ellingsen, K.,
477 Gauss, M., Hauglustaine, D. A., Isaksen, I. S. A., Lawrence, M. G., Richter, A., Rodriguez, J. M.,
478 Sanderson, M., Strahan, S. E., Sudo, K., Szopa, S., van Noije, T. P. C. and Wild, O.: Multi-model
479 simulations of the impact of international shipping on Atmospheric Chemistry and Climate in
480 2000 and 2030, Atmos. Chem. Phys., 7, 757–780, 2007.

481 Fiore, A. M., Naik, V., Spracklen, D. V., Steiner, A., Unger, N., Prather, M., Bergmann, D.,
482 Cameron-Smith, P. J., Cionni, I., Collins, W. J., Dalsoren, S., Eyring, V., Folberth, G. A.,
483 Ginoux, P., Horowitz, L. W., Josse, B., Lamarque, J.-F., MacKenzie, I. A., Nagashima, T.,
484 O'Connor, F. M., Righi, M., Rumbold, S. T., Shindell, D. T., Skeie, R. B., Sudo, K., Szopa, S.,
485 Takemura, T. and Zeng, G.: Global air quality and climate, Chem. Soc. Rev., 41(19), 6663–6683,
486 doi:10.1039/c2cs35095e, 2012.

487 Franke, K., Eyring, V., Sander, R., Hendricks, J., Lauer, A. and Sausen, R.: Toward effective
488 emissions of ships in global models, Meteorol. Z., 17(2), 117–129, doi:10.1127/0941-
489 2948/2008/0277, 2008.

490 Fuglestvedt, J., Berntsen, T., Myhre, G., Rypdal, K. and Skeie, R. B.: Climate forcing from the
491 transport sectors, P. Natl. Acad. Sci. USA, 105(2), 454–458, doi:10.1073/pnas.0702958104,
492 2008.

493 Galmarini, S., Dearellano, J. and Duynkerke, P. G.: The effect of microscale turbulence on the
494 reaction-rate in a chemically reactive plume, Atmos. Environ., 29(1), 87–95, 1995.

495 Granier, C., Bessagnet, B., Bond, T., D'Angiola, A., van der Gon, H. D., Frost, G. J., Heil, A.,
496 Kaiser, J. W., Kinne, S., Klimont, Z., Kloster, S., Lamarque, J.-F., Liousse, C., Masui, T.,
497 Meleux, F., Mieville, A., Ohara, T., Raut, J.-C., Riahi, K., Schultz, M. G., Smith, S. J.,
498 Thompson, A., van Aardenne, J., van der Werf, G. R. and van Vuuren, D. P.: Evolution of
499 anthropogenic and biomass burning emissions of air pollutants at global and regional scales
500 during the 1980-2010 period, Climatic Change, 109, 163–190, doi:10.1007/s10584-011-0154-1,
501 2011.

Hodnebrog, O., Berntsen, T. K., Dessens, O., Gauss, M., Grewe, V., Isaksen, I. S. A., Koffi, B., Myhre, G., Olivie, D., Prather, M. J., Pyle, J. A., Stordal, F., Szopa, S., Tang, Q., van Velthoven, P., Williams, J. E. and Odemark, K.: Future impact of non-land based traffic emissions on atmospheric ozone and OH - an optimistic scenario and a possible mitigation strategy, Atmos. Chem. Phys., 11(21), 11293–11317, doi:10.5194/acp-11-11293-2011, 2011.

Holmes, C. D., Prather, M. J., Søvde, O. A. and Myhre, G.: Future methane, hydroxyl, and their uncertainties: key climate and emission parameters for future predictions, Atmos. Chem. Phys., 13(1), 285–302, doi:10.5194/acp-13-285-2013, 2013.

Holmes, C. D., Tang, Q. and Prather, M. J.: Uncertainties in climate assessment for the case of aviation NO, P. Natl. Acad. Sci. USA, 108(27), 10997–11002, doi:10.1073/pnas.1101458108, 2011.

Hoor, P., Borken-Kleefeld, J., Caro, D., Dessens, O., Endresen, O., Gauss, M., Grewe, V., Hauglustaine, D., Isaksen, I. S. A., Jockel, P., Lelieveld, J., Myhre, G., Meijer, E., Olivie, D., Prather, M., Schnadt Poberaj, C., Shine, K. P., Staehelin, J., Tang, Q., van Aardenne, J., van Velthoven, P. and Sausen, R.: The impact of traffic emissions on atmospheric ozone and OH: results from QUANTIFY, Atmos. Chem. Phys., 9(9), 3113–3136, 2009.

Huszar, P., Cariolle, D., Paoli, R. and Halenka, T.: Modeling the regional impact of ship emissions on NOx and ozone levels over the Eastern Atlantic and Western Europe using ship plume parameterization, Atmos. Chem. Phys., 10, 6645–6660, doi:10.5194/acp-10-6645-2010, 2010.

Jaeglé, L., Quinn, P. K., Bates, T. S., Alexander, B. and Lin, J.-T.: Global distribution of sea salt aerosols: new constraints from in situ and remote sensing observations, Atmos. Chem. Phys., 11, 3137–3157, doi:10.5194/acp-11-3137-2011, 2011.

Kasibhatla, P., Levy, H., Moxim, W. J., Pandis, S. N., Corbett, J. J., Peterson, M. C., Honrath, R. E., Frost, G. J., Knapp, K., Parrish, D. D. and Ryerson, T. B.: Do emissions from ships have a significant impact on concentrations of nitrogen oxides in the marine boundary layer? Geophys. Res. Lett., 27(15), 2229–2232, 2000.

Kim, H. S., Song, C. H., Park, R. S., Huey, G. and Ryu, J. Y.: Investigation of ship-plume chemistry using a newly-developed photochemical/dynamic ship-plume model, Atmos. Chem. Phys., 9(19), 7531–7550, 2009.

Koffi, B., Szopa, S., Cozic, A., Hauglustaine, D. and van Velthoven, P.: Present and future impact of aircraft, road traffic and shipping emissions on global tropospheric ozone, Atmos. Chem. Phys., 10(23), 11681–11705, doi:10.5194/acp-10-11681-2010, 2010.

Lamarque, J.-F., Bond, T. C., Eyring, V., Granier, C., Heil, A., Klimont, Z., Lee, D., Liousse, C., Mieville, A., Owen, B., Schultz, M. G., Shindell, D., Smith, S. J., Stehfest, E., van Aardenne, J., Cooper, O. R., Kainuma, M., Mahowald, N., McConnell, J. R., Naik, V., Riahi, K. and van Vuuren, D. P.: Historical (1850-2000) gridded anthropogenic and biomass burning emissions of reactive gases and aerosols: methodology and application, Atmos. Chem. Phys., 10(15), 7017–7039, doi:10.5194/acp-10-7017-2010, 2010.

Lawrence, M. G. and Crutzen, P. J.: Influence of NOx emissions from ships on tropospheric photochemistry and climate, Nature, 402(6758), 167–170, 1999.

543 Lee, C., Martin, R. V., van Donkelaar, A., Lee, H., Dickerson, R. R., Hains, J. C., Krotkov, N.,
544 Richter, A., Vinnikov, K. and Schwab, J. J.: SO2 emissions and lifetimes: Estimates from inverse
545 modeling using in situ and global, space-based (SCIAMACHY and OMI) observations, J.
546 Geophys. Res.-Atmos., 116, D06304, doi:10.1029/2010JD014758, 2011.

547 Lee, D. S., Lim, L., Eyring, V., Sausen, R., Endresen, O. and Behrens, H.-L.: Radiative forcing
548 and temperature response from shipping, in Proceedings of an International Conference on
549 Transport, Atmosphere and Climate (TAC), edited by R. Sausen, A. Blum, D. S. Lee, and C.
550 Brüning, Office for Official Publications of the European Communities, Luxembourg, 208–213.
551 available at: http://www.pa.op.dlr.de/tac/2006/proceedings.html (last access: 8 August 2012),
552 2007.

553 Leibensperger, E. M., Mickley, L. J. and Jacob, D. J.: Intercontinental influence of NOx and CO
554 emissions on particulate matter air quality, Atmos. Environ., 45, 3318–3324,
555 doi:10.1016/j.atmosenv.2011.02.023, 2011.

556 Lin, X., Trainer, M. and Liu, S. C.: On the nonlinearity of the tropospheric ozone production, J.
557 Geophys. Res.-Atmos., 93(D12), 15879–15888, 1988.

558 Murray, L. T., Jacob, D. J., Logan, J. A., Hudman, R. C. and Koshak, W. J.: Optimized regional
559 and interannual variability of lightning in a global chemical transport model constrained by
560 LIS/OTD satellite data, J. Geophys. Res.-Atmos., 117, D20307, doi:10.1029/2012JD017934,
561 2012.

562 Myhre, G., Nilsen, J. S., Gulstad, L., Shine, K. P., Rognerud, B. and Isaksen, I. S. A.: Radiative
563 forcing due to stratospheric water vapour from CH_4 oxidation, Geophys. Res. Lett., 34(1),
564 L01807, doi:10.1029/2006GL027472, 2007.

565 Myhre, G., Samset, B. H. and Schulz, M.: Radiative forcing of the direct aerosol effect from
566 AeroCom Phase II simulations, Atmos. Chem. Phys., 13, 1853–1877, doi:10.5194/acp-13-1853-
567 2013, 2013.

568 Myhre, G., Shine, K. P., Raedel, G., Gauss, M., Isaksen, I. S. A., Tang, Q., Prather, M. J.,
569 Williams, J. E., van Velthoven, P., Dessens, O., Koffi, B., Szopa, S., Hoor, P., Grewe, V.,
570 Borken-Kleefeld, J., Berntsen, T. K. and Fuglestvedt, J. S.: Radiative forcing due to changes in
571 ozone and methane caused by the transport sector, Atmos. Environ., 45(2), 387–394,
572 doi:10.1016/j.atmosenv.2010.10.001, 2011.

573 Naik, V., Voulgarakis, A., Fiore, A. M., Horowitz, L. W., Lamarque, J. F., Lin, M., Prather, M. J.,
574 Young, P. J., Bergmann, D., Cameron-Smith, P. J., Cionni, I., Collins, W. J., Dalsøren, S. B.,
575 Doherty, R., Eyring, V., Faluvegi, G., Folberth, G. A., B, J., Lee, Y. H., MacKenzie, I. A.,
576 Nagashima, T., van Noije, T. P. C., Plummer, D. A., Righi, M., Rumbold, S. T., Skeie, R.,
577 Shindell, D. T., Stevenson, D. S., Strode, S., Sudo, K., Szopa, S. and Zeng, G.: Preindustrial to
578 present-day changes in tropospheric hydroxyl radical and methane lifetime from the Atmospheric
579 Chemistry and Climate Model Intercomparison Project (ACCMIP), Atmos. Chem. Phys., 13(10),
580 5277–5298, doi:10.5194/acp-13-5277-2013, 2013.

581 Olivie, D. J. L., Cariolle, D., Teyssedre, H., Salas, D., Voldoire, A., Clark, H., Saint-Martin, D.,
582 Michou, M., Karcher, F., Balkanski, Y., Gauss, M., Dessens, O., Koffi, B. and Sausen, R.:
583 Modeling the climate impact of road transport, maritime shipping and aviation over the period
584 1860-2100 with an AOGCM, Atmos. Chem. Phys., 12(3), 1449–1480, doi:10.5194/acp-12-1449-

2012, 2012.

Olivier, J. G. J. and Berdowski, J.: Global emissions sources and sinks, in The Climate System, edited by J. Berdowski, R. Guicherit, and B. J. Heij, pp. 33–78, A A Balkema Publishers/Swets & Zeitlinger Publishers, Lisse, The Netherlands. 2001.

Paoli, R., Cariolle, D. and Sausen, R.: Review of effective emissions modeling and computation, Geosci. Model Dev., 4(3), 643–667, doi:10.5194/gmd-4-643-2011, 2011.

Parrella, J. P., Jacob, D. J., Liang, Q., Zhang, Y., Mickley, L. J., Miller, B., Evans, M. J., Yang, X., Pyle, J. A., Theys, N. and Van Roozendael, M.: Tropospheric bromine chemistry: implications for present and pre-industrial ozone and mercury, Atmos. Chem. Phys., 12(15), 6723–6740, doi:10.5194/acp-12-6723-2012, 2012.

Parrish, D. D., Millet, D. B. and Goldstein, A. H.: Increasing ozone in marine boundary layer inflow at the west coasts of North America and Europe, Atmos. Chem. Phys., 9, 1303–1323, 2009.

Paxian, A., Eyring, V., Beer, W., Sausen, R. and Wright, C.: Present-day and future global bottom-up ship emission inventories including polar routes, Environ. Sci. Technol., 44(4), 1333–1339, doi:10.1021/es9022859, 2010.

Prather, M., Holmes, C. and Hsu, J.: Reactive greenhouse gas scenarios: Systematic exploration of uncertainties and the role of atmospheric chemistry, Geophys. Res. Lett., 39, L09803, doi:10.1029/2012GL051440, 2012.

Rienecker, M. M., Suarez, M. J., Todling, R., Bacmeister, J., Takacs, L., Liu, H.-C., Gu, W., Sienkiewicz, M., Koster, R. D., Gelaro, R., Stajner, I. and Nielsen, J. E.: The GEOS-5 Data Assimilation System, Technical Report Series on Global Modeling and Data Assimilation. 2008.

Sillman, S., Logan, J. A. and Wofsy, S. C.: A regional scale model for ozone in the United States with subgrid representation of urban and power plant plumes, J. Geophys. Res.-Atmos., 95(D5), 5731, doi:10.1029/JD095iD05p05731, 1990.

Song, C. H., Chen, G., Hanna, S. R., Crawford, J. and Davis, D. D.: Dispersion and chemical evolution of ship plumes in the marine boundary layer: Investigation of $O_3/NO_y/HO_x$ chemistry, J. Geophys. Res.-Atmos., 108(D4), 4143, doi:10.1029/2002JD002216, 2003.

Sykes, R. I., Henn, D. S., Parker, S. F. and Lewellen, W. S.: Large-eddy simulation of a turbulent reacting plume, Atmos. Environ., 26(14), 2565–2574, 1992.

Unger, N., Bond, T. C., Wang, J. S., Koch, D. M., Menon, S., Shindell, D. T. and Bauer, S.: Attribution of climate forcing to economic sectors, P. Natl. Acad. Sci. USA, 107(8), 3382–3387, doi:10.1073/pnas.0906548107, 2010.

van Aardenne, J. A., Dentener, F., Olivier, J. G. J., Peters, J. A. H. W. and Ganzeveld, L. N.: The EDGAR 3.2 Fast Track 2000 Dataset (32FT2000), Emission Database for Global Atmospheric Research (EDGAR) Consortium, available at: http://themasites.pbl.nl/images/Description_of_EDGAR_32FT2000(v8)_tcm61-46462.pdf (last access: 15 October 2013), 2005.

van Donkelaar, A., Martin, R. V., Leaitch, W. R., Macdonald, A. M., Walker, T. W., Streets, D. G., Zhang, Q., Dunlea, E. J., Jimenez, J. L., Dibb, J. E., Huey, L. G., Weber, R. and Andreae, M. O.: Analysis of aircraft and satellite measurements from the Intercontinental Chemical Transport Experiment (INTEX-B) to quantify long-range transport of East Asian sulfur to Canada, Atmos. Chem. Phys., 8(11), 2999–3014, doi:10.5194/acp-8-2999-2008, 2008.

van het Bolscher, M.: REanalysis of the TROpospheric chemical composition over the past 40 years: A long-term global modeling study of tropospheric chemistry funded under the 5th EU framework programme, Max Planck Institute for Meteorology, Hamburg, Germany. 2008.

Verzijlbergh, R. A., Jonker, H. J. J., Heus, T. and de Arellano, J. V.-G.: Turbulent dispersion in cloud-topped boundary layers, Atmos. Chem. Phys., 9(4), 1289–1302, 2009.

Vinken, G. C. M., Boersma, K. F., Jacob, D. J. and Meijer, E. W.: Accounting for non-linear chemistry of ship plumes in the GEOS-Chem global chemistry transport model, Atmos. Chem. Phys., 11(22), 11707–11722, doi:10.5194/acp-11-11707-2011, 2011.

Vinken, G. C. M., Boersma, K. F., van Donkelaar, A. and Zhang, L.: Constraints on ship NO_x emissions in Europe using GEOS-Chem and OMI satellite NO_2 observations, Atmos. Chem. Phys., 13(7), 19351–19388, doi:10.5194/acpd-13-19351-2013, 2013.

von Glasow, R., Lawrence, M. G., Sander, R. and Crutzen, P. J.: Modeling the chemical effects of ship exhaust in the cloud-free marine boundary layer, Atmos. Chem. Phys., 3, 233–250, 2003.

Wang, C., Corbett, J. J. and Firestone, J.: Improving Spatial Representation of Global Ship Emissions Inventories, Environ. Sci. Technol., 42(1), 193–199, doi:10.1021/es0700799, 2008.

Wang, Q., Jacob, D. J., Fisher, J. A., Mao, J., Leibensperger, E. M., Carouge, C. C., Le Sager, P., Kondo, Y., Jimenez, J. L., Cubison, M. J. and Doherty, S. J.: Sources of carbonaceous aerosols and deposited black carbon in the Arctic in winter-spring: implications for radiative forcing, Atmos. Chem. Phys., 11(23), 12453–12473, doi:10.5194/acp-11-12453-2011, 2011.

Wild, O. and Prather, M. J.: Global tropospheric ozone modeling: Quantifying errors due to grid resolution, J. Geophys. Res.-Atmos., 111(D11), D11305, doi:10.1029/2005JD006605, 2006.

651 **Table 1. Radiative efficiency of O_3 generated from ship NO_x**

Source	Value or range, mW m^{-2} DU^{-1}
Eyring et al. (2007)	33.2-33.7[a,b]
Fuglestvedt et al. (2008)	27.8[a]
Hoor et al. (2009)	36.7 ± 3.0[b,c]
Myhre et al. (2011)	30.1 ± 1.6[b,c]
This work	33.0 ± 4[d]

652 [a] Calculated by removing all ship NO_x emissions.

653 [b] Derived from reported O_3 burden and RF.

654 [c] Calculated for 5% perturbation to year 2000 ship NO_x emissions.

655 [d] Average of models used by Hoor et al. (2009) and Myhre et al. (2011).

656

Table 2: Effect of ship NO_x emissions on O_3 column and RF.[a]

	Instant dilution		Fixed OPE		Parametric plume chemistry	
	$\frac{d[O_3]}{dE}$	$\frac{dF_{O_3}}{dE}$	$\frac{d[O_3]}{dE}$	$\frac{dF_{O_3}}{dE}$	$\frac{d[O_3]}{dE}$	$\frac{dF_{O_3}}{dE}$
This work						
GEOS-Chem[b]	0.16	5.3	0.12	3.8	0.10	3.4
Holmes et al. (2013)						
GEOS-Chem[c,d]			0.12	3.8		
UCI CTM[d]	0.17	5.6				
Oslo CTM3[d]	0.23	7.7				
Literature						
models[e]	0.18 ± 0.04	6.0 ±1.9				

[a] $d[O_3]/dE$ is the derivative of ozone column density with respect to ship NO_x emissions, reported in DU [Tg(N) yr^{-1}]$^{-1}$. dF_{O3}/dE is the derivative of O_3 RF with respect to ship NO_x emissions, reported in mW m^{-2} [Tg(N) yr^{-1}]$^{-1}$. Both $d[O_3]/dE$ and dF_{O3}/dE are calculated from steady-state 5% perturbations to ship NO_x emissions on top of the base emission inventory.

[b] Emissions as described in Section 2. Ship NO_x emissions are 5.0 Tg(N) yr^{-1}.

[c] Holmes et al. (2013) used GEOS-Chem version 9-01-02, while this work uses version 9-01-03.

[d] Configured as described by Holmes et al. (2013), using Representative Concentration Pathway (RCP) emissions for year 2000. These include 5.4 Tg(N) yr^{-1} from ships.

[e] From modeling studies by Endresen et al. (2003), Hoor et al. (2009), Dalsoren et al. (2010), Borken-Kleefeld et al. (2010), Unger et al. (2010), Myhre et al. (2011), Olivie et al. (2012), Dalsoren et al. (2013), and Eide et al. (2013) excluding Lee et al. (2007) and Eyring et al. (2007) for reasons given in Section 4. Emission inventories and perturbation magnitudes differ, but all assume instant dilution.

672 **Table 3: Effect of ship NO_x emissions on CH_4 lifetime and RF.[a]**

	Instant dilution			Fixed OPE			Parametric plume chemistry		
	τ	$\frac{d\ln\tau}{dE}$	$\frac{dF_{CH_4}}{dE}$	τ	$\frac{d\ln\tau}{dE}$	$\frac{dF_{CH_4}}{dE}$	τ	$\frac{d\ln\tau}{dE}$	$\frac{dF_{CH_4}}{dE}$
This work									
GEOS-Chem[b]	9.2	-1.0	-8.5	9.7	-0.26	-2.2	9.4	-0.7	-5.7
Holmes et al. (2013)									
GEOS-Chem[c,d]				10.0	-0.31	-2.6			
UCI CTM[c]	8.5	-0.8	-6.8						
Oslo CTM3[c]	8.7	-0.9	-7.6						
Literature									
models[e]		-0.9±0.3	-8.0±2.4						
observations[f]	11.2±1.3			11.2±1.3			11.2±1.3		

673 [a] τ is the CH_4 lifetime due to tropospheric OH, reported in years. $(d\ln\tau)/dE$ is the derivative of τ
674 with respect to ship NO_x emissions, reported in % [Tg(N) yr^{-1}]$^{-1}$. dF_{CH4}/dE is the derivative of
675 CH_4 RF with respect to ship NO_x emissions, reported in mW m^{-2} [Tg(N) yr^{-1}]$^{-1}$. Both $d\tau/dE$ and
676 dF_{CH4}/dE are calculated from steady-state 5% perturbations to ship NO_x emissions on top of the
677 base emission inventory.
678 [b] Emissions as described in Section 2. Ship NO_x emissions are 5.0 Tg(N) yr^{-1}.
679 [c] Holmes et al. (2013) used GEOS-Chem version 9-01-02, while this work uses version 9-01-03.
680 [d] Configured as described by Holmes et al. (2013), using Representative Concentration Pathway
681 (RCP) emissions for year 2000. These include 5.4 Tg(N) yr^{-1} from ships.
682 [e] From modeling studies used in Table 2, plus Lawrence and Crutzen (1999), Dalsoren et al.
683 (2007), Dalsoren et al. (2009), and Hodnebrog et al. (2011). Emission inventories and
684 perturbation magnitudes differ, but all assume instant dilution.
685 [f] From observations of methyl chloroform (Prather et al., 2012).

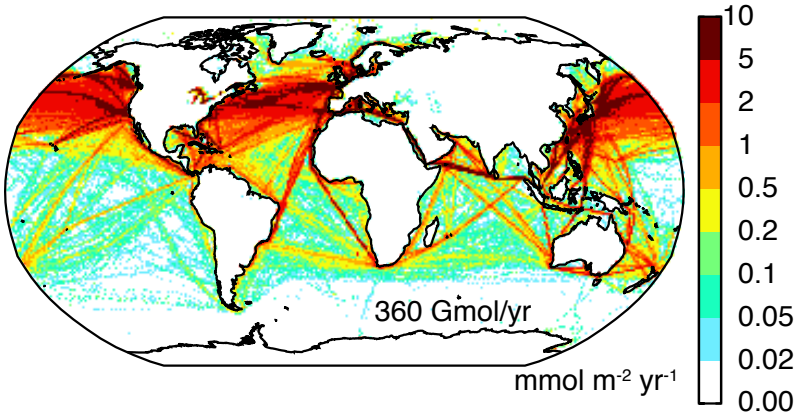

686

687 **Figure 1:**

688 Annual ship NO_x emissions (mmol m^{-2} yr^{-1}) used in GEOS-Chem. The CTM includes monthly
689 variations in locations and magnitude (not shown).

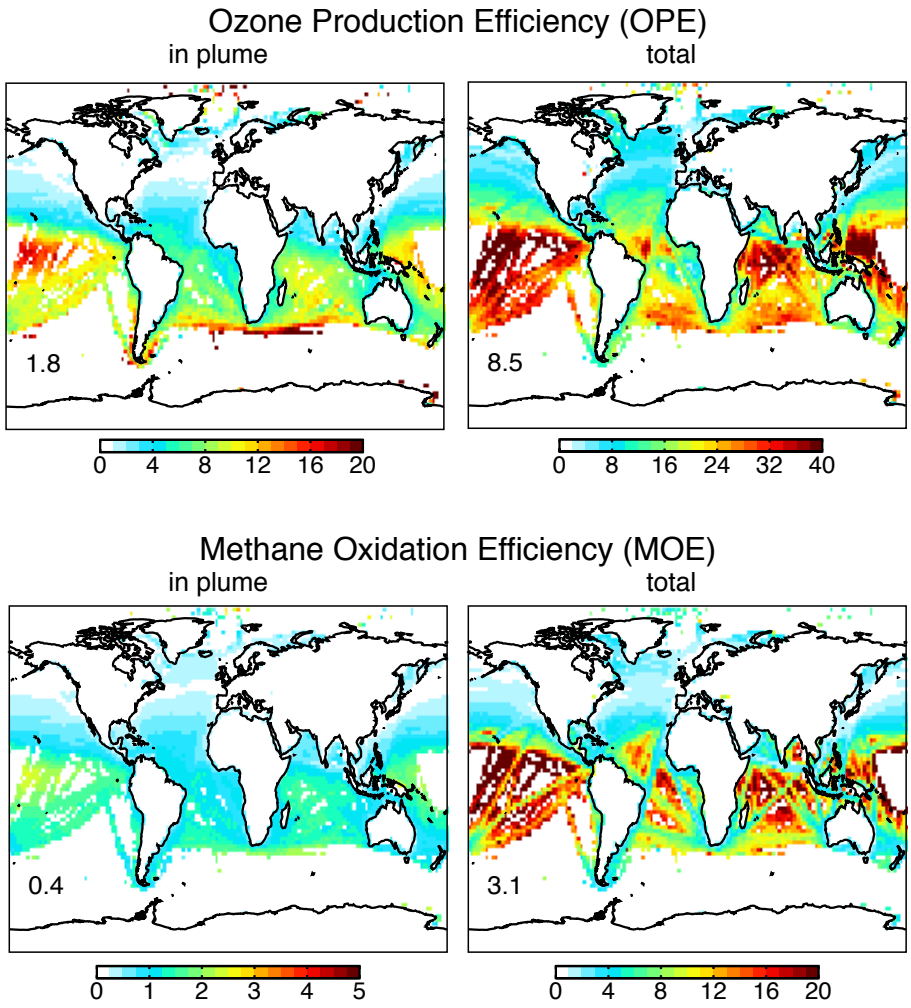

690

691 **Figure 2:**

692 Time-averaged ozone production efficiency (top row) and methane oxidation efficiency
693 (bottom row) for marginal increases in ship NO_x emissions within the sub-grid plume (left panels)
694 and total (plume plus grid chemistry, right panels). Values are shown from the CTM with
695 parametric plume chemistry only where ship NO_x emissions exceed 10^4 molec m^{-2} s^{-1}. Inset
696 numbers give global averages.

697

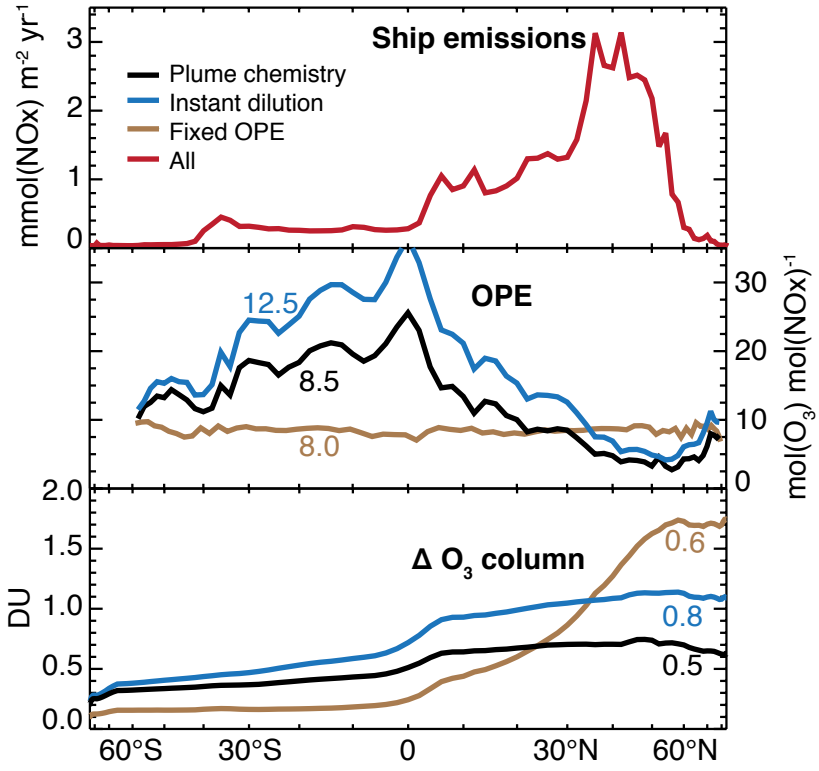

698

699 **Figure 3:**

700 Annual and zonal-mean NO_x emission and ozone changes caused by maritime shipping plotted
701 against sine latitude for each plume dilution assumption. OPE is averaged over regions where
702 ship NO_x emissions exceed 10^4 molec m^{-2} s^{-1}. Ozone column changes (ΔO_3) are calculated from
703 5% perturbations to full ship emissions, then multiplied by 20. Inset numbers give global
704 averages.

705

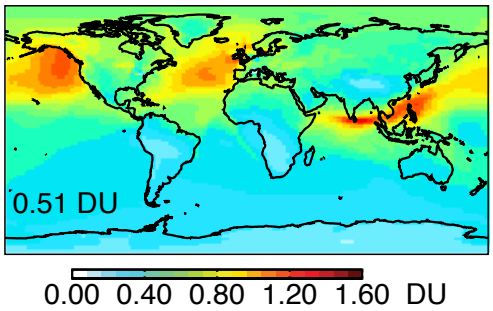

706

707 **Figure 4:**

708 Annual-mean O_3 column enhancements due to ship NO_x emissions with parametric plume
709 chemistry. Values are calculated from a 5% emission perturbation and multiplied by 20. Inset
710 number gives the global-mean change. Patterns are similar in the instant dilution simulation, but
711 with fixed OPE, the O_3 enhancements shift toward high northern latitudes (Fig. 3).

712

713

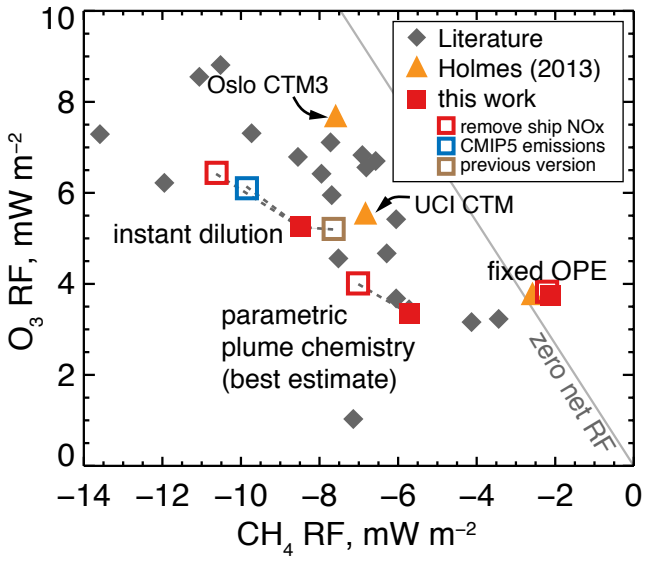

714

715 **Figure 5.**

716 Steady-state RF (mW m^{-2}) from O_3 and CH_4 caused by ship NO_x emissions. Values are scaled
717 to emissions of 1 Tg(N) yr^{-1}. Dashed lines link estimates that are made with 5% increases in ship
718 NO_x (filled squares) to others made with the same plume dilution and chemistry assumption
719 (open squares). These other estimates use CMIP5 emissions, a previous GEOS-Chem model
720 version, and complete removal of ship NO_x emissions. The zero net RF line accounts for long-
721 lived O_3 changes that enhance the CH_4 RF by approximately 34% (Eq. 4). Literature values are
722 from studies listed in Tables 2 and 3.